

# High-Conversion-Ratio Bidirectional DC–DC Converter with Dual Coupled Inductors

Omid Khezri\*, Javad Javidan

Technical Engineering Department, University of Mohaghegh Ardabili, Ardabil, Iran

\*Corresponding author, e-mail: omidkhezri0055@gmail.com

## Abstract

*In this paper, a high-conversion-ratio bidirectional DC–DC converter with dual coupled inductors is proposed. In the boost mode, two capacitors are parallel charged and series discharged by the dual coupled inductors. Thus, high step-up voltage gain can be achieved with an appropriate duty ratio. In the buck mode, two capacitors are series charged and parallel discharged by the dual coupled inductors. The bidirectional converter can have high step-down voltage gain. The stress voltage of all switches can be reduced, and the switching loss and efficiency can be improved. The operating principle and the steady-state analyses of the voltage gain are discussed. Finally, in 24V for low voltage, and 400V for high voltage, and 200W for output power, this converter simulated in MATLAB.*

**Keywords:** Bidirectional, DC-DC converter, dual coupled inductors, high conversion ratio

## 1. Introduction

Renewable energy systems are more widely used in the world such as solar and wind energy [1]-[3]. However, photovoltaic (PV) solar or wind power cannot provide sufficient power when the load is suddenly increased [4]-[6]. Because the renewable systems cannot provide a stable power for user, the renewable energy systems and battery can be employed for the hybrid power systems [7]. When the renewable energy systems cannot supply enough power for the load, the battery must provide this power. If the power of the renewable energy systems cannot be used completely by the load, the excess energy can be used to charge the battery [8]-[10]. Because the bidirectional DC–DC converters can transfer the power between two DC sources in either direction, these converters are widely used for renewable energy hybrid power systems, hybrid electric vehicle energy systems and uninterrupted power supplies [11]-[12]. The topologies of these converters have the isolated and non-isolated types for different applications. The isolated types include the flyback type [13]-[14], forward-flyback type [15]-[16], half-bridge type [17]-[18] and full-bridge type [19]. These converters can achieve high voltage gain by adjusting the turns ratio of the transformer. The bidirectional flyback converter has the simple structure and easy control but the switches of this converter have high voltage stresses. Thus, this converter is applied for low power applications. To reduce the voltage stresses on the switches, the energy regeneration techniques used [20]. The non-isolated types include the multi-level type, switched-capacitor type, cuk/cuk type, sepic/zeta type, buck-boost type, coupled-inductor type, three-level type and conventional buck/boost type [21]. In multi-level and switched-capacitor types, if high voltage gain is needed, more switches and capacitors are required. Also, the control circuits of these converters are complicated. For the cuk/cuk and sepic/zeta types, the efficiency is low because these converters cannot provide wide voltage conversion range [22]-[24]. The converter in [25] has the high conversion ratio but this converter is unidirectional. Compare with [25], the proposed converter successfully developed to bidirectional dc-dc converter with a dual coupled inductors, and the switches voltage stress is reduced and efficiency is increased in boost and buck mode.

The proposed bidirectional converter is analysed, and its operation in boost and buck mode is described in section II. Steady-state analysis and equations of the boost and buck mode are described in section III and simulation results are described in section IV.

## 2. Operating Principle OfThe Proposed Converter

Figure 1 shows the circuit topology of the proposed converter. This converter consists of the dc input voltage  $V_L$ , the power switch  $S_1, S_2, S_7$ , two capacitors  $C_1$  and  $C_2$ , and the dual coupled inductors  $N_P$  and  $N_S$ .

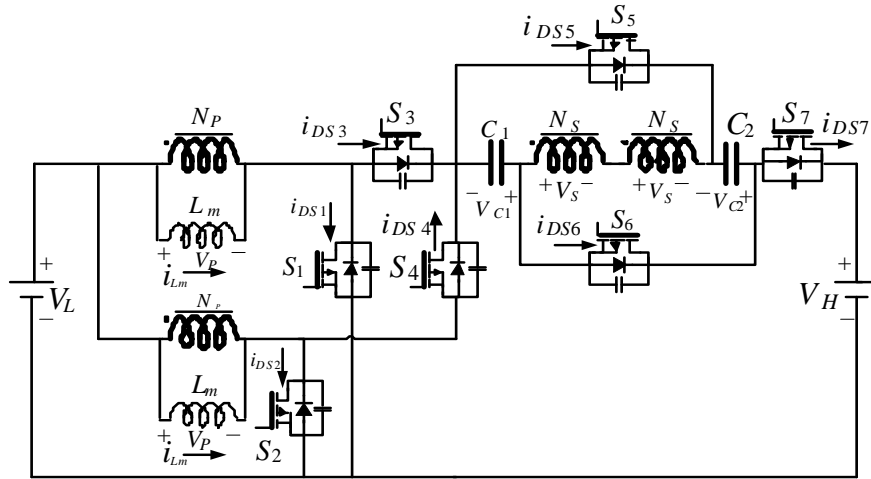


Figure 1. Circuit configuration of the bidirectional converter

In the boost mode, parallel-charged and series-discharged capacitors can achieve high step-up gain. Also in the buck mode, series-charged and parallel-discharged capacitors can achieve high step-down gain. In the boost mode operation,  $S_1, S_2$  is the main switch. The voltage across switches  $S_1, S_2$  can be reduced. Since switches  $S_1, S_2$  has a low voltage level, the low conducting resistance  $R_{DS(ON)}$  of the switch is used to reduce the conduction loss. In the buck mode operation, the coupled inductors are used as a transformer. Thus, two capacitors  $C_1$  and  $C_2$  can be series-charged by high voltage side and parallel-discharged through the secondary side. The main switches are  $S_3, S_4$  and  $S_7$ . The switching loss is improved and the efficiency can be increased.

### A. Boost-mode Operation

Figure 2(a) shows the waveforms and Figure 3 shows the current flow path of the proposed converter in boost mode. There are two operating modes in one switching period of the proposed converter. The main switch is  $S_1, S_2$  for each mode. The operating modes are described as Figure 2.

- 1) Mode I [ $t_0 - t_1$ ]:  $S_1, S_2, S_5, S_6$  turn on and  $S_3, S_4, S_7$  turn off in  $t = t_0$ . The current-flow path is shown in Fig. 3(a). The dc source  $V_L$  charges the magnetizing inductor  $L_m$ , and the charging capacitors  $C_1$  and  $C_2$  via the dual coupled inductors. Voltages  $V_{C1}$  and  $V_{C2}$  are equal to  $2nV_L$  and two capacitors are charged in parallel. The output capacitor  $C_H$  provides energy to load  $R$ . This operating mode ends when switch  $S_1, S_2$  is turned off at  $t = t_1$ .
- 2) Mode II [ $t_1 - t_2$ ]:  $S_3, S_4, S_7$  turn on and  $S_1, S_2, S_5, S_6$  turn off. The current flow path is shown in Figure 3(b). The dual coupled inductors, dc source  $V_L$ , and capacitors  $C_1$  and  $C_2$  are connected in series to charge the output capacitor  $C_H$  and load  $R$ . This operating mode ends when switch  $S_3, S_4, S_7$  is turned off at  $t = t_2$  and beginning of the next switching period.

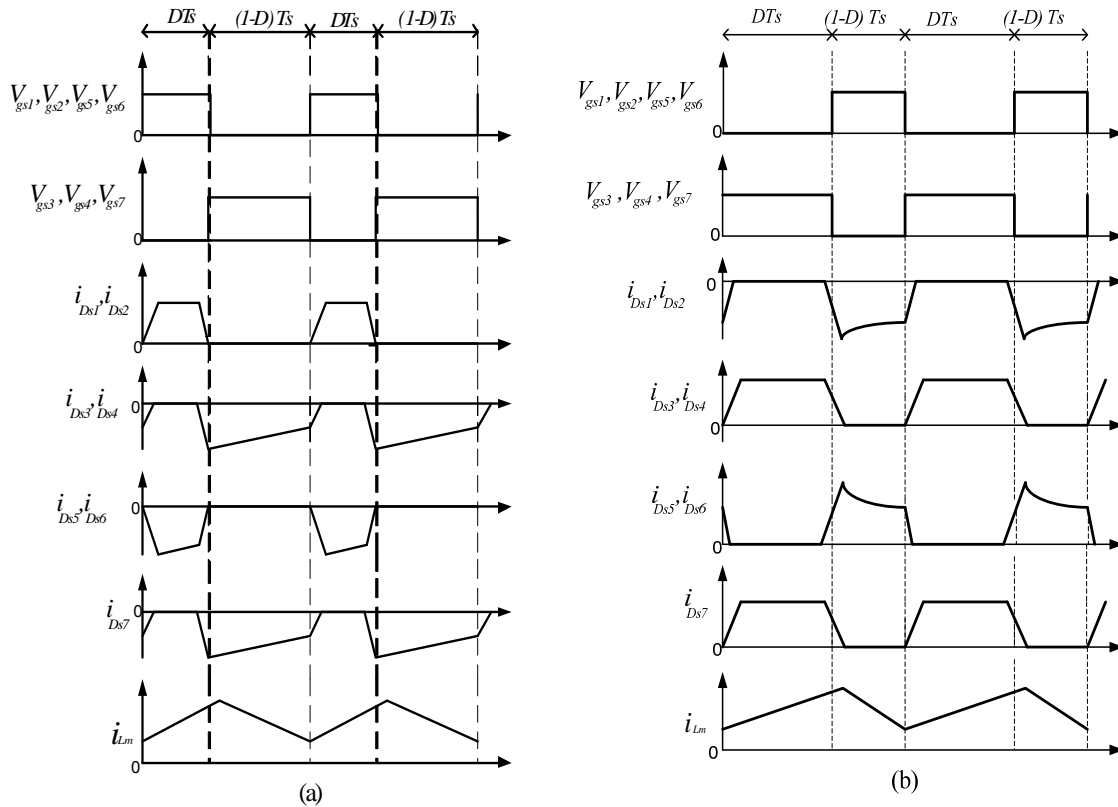


Figure 2. Waveforms of the bidirectional converter. (a) boost mode, (b) buck mode

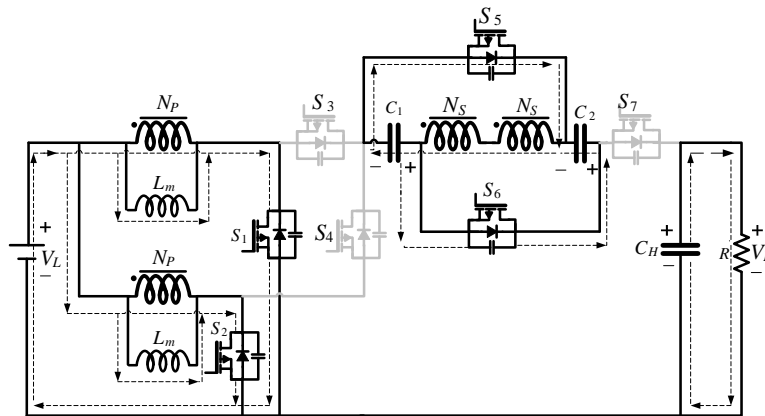


Figure 3. Current-flow path of the operating mode during one switching period in the boost mode

**B. Buck-mode Operation**

Figure 2(b) shows the waveforms, and Figure 7 shows the current flow path for each mode. The operating modes are described below.

- 1) Mode I [ $t_0 - t_1$ ]:  $S_3, S_4, S_7$  turn on and  $S_1, S_2, S_5, S_6$  turn off. The current flow path is shown in Figure 4(a). Capacitors  $C_1, C_2$  and the secondary side coil  $N_S$  are still charged in series by  $V_H$ , and the magnetizing inductor  $L_m$  is also charged. The output capacitor  $C_L$  provide the energy to load  $R$ . This operating mode ends when switch  $S_3, S_4, S_7$  is turned off at  $t = t_1$ .

- 2) Mode II [ $t_1 - t_2$ ]:  $S_1, S_2, S_5, S_6$  turn on and  $S_3, S_4, S_7$  turn off at  $t = t_1$ . The current flow path is shown in Figure 4(b). The energy of capacitors  $C_1$  and  $C_2$  discharges to the output capacitor  $C_L$  and load  $R$  through the dual coupled inductors. The magnetizing inductor  $L_m$  also discharges to the output. This operating mode ends when switch  $S_1, S_2$  is turned off at  $t = t_2$ .

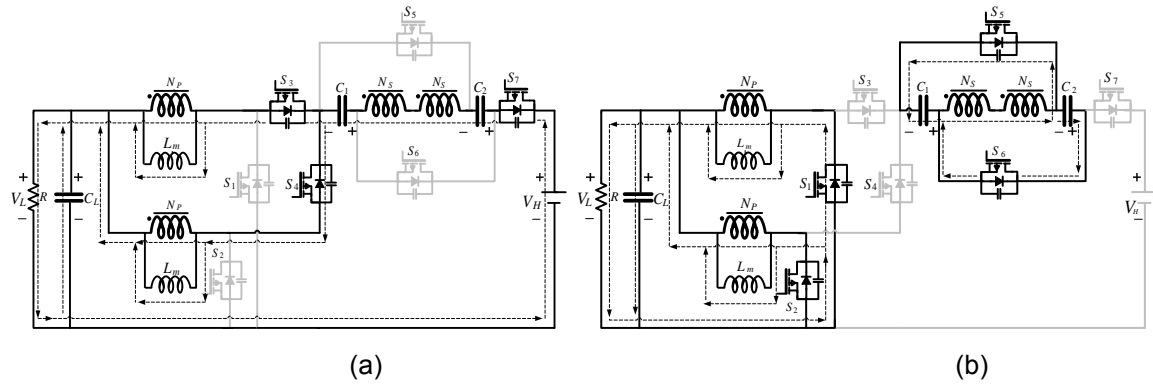


Figure 4. Current-flow path of the operating mode during one switching period in the buckmode

**3. Steady-State Analysis of the Proposed Converter**

After the mode analysis of the boost and buck mode operations, the following equations and voltage gain in the steady state of the proposed converter can be derived. The equations of the turnratio of the coupled inductor are defined as

$$n = \frac{N_s}{N_p} \tag{1}$$

**A. Boost-mode Operation**

There are two operating modes in one switching period of the proposed converter. In the time period of mode I, the following equations can be written based on Figure 3(a). The voltage on the primary and secondary sides of the dual coupled inductors are shown as

$$V_p^I = V_L \tag{2}$$

$$V_s^I = nV_p^I = nV_L \tag{3}$$

Also the voltage of capacitors  $C_1$  and  $C_2$  can be written as follows:

$$V_{c1} = V_{c2} = 2V_s^I = 2nV_L \tag{4}$$

Based on Figure 3(b), in modes II, the voltage on the secondary side of the dual coupled inductors can be formulated as follows:

$$2V_s^{II} = V_L - V_p^{II} + V_{c1} + V_{c2} - V_H \tag{5}$$

$$2nV_p^{II} = V_L - V_p^{II} + 4nV_L - V_H \tag{6}$$

$$V_p^{II} = \frac{(1 + 4n)V_L - V_H}{1 + 2n} \tag{7}$$

Using the volt-second balance principle on the magnetizing inductor  $L_m$ , the following is given:

$$\int_0^{DT_s} V_p^I dt + \int_{DT_s}^{T_s} V_p^{II} dt = 0 \tag{8}$$

Also, the voltage stress of the main switch  $S_1, S_2$  can be expressed as

$$V_p^{II} = V_L - V_{s1,s2} \quad (9)$$

Substituting (2) and (9) into (8), voltage stress is obtained as

$$V_{DS1,DS2} = \frac{V_L}{1-D} \quad (10)$$

Substituting (2) and (7) into (8), the voltage gain of the boost state operation is obtained as

$$M_{\text{boost}} = \frac{V_H}{V_L} = \frac{1+4n-2Dn}{1-D} \quad (11)$$

### B. Buck-mode Operation

In the time period of mode I, the following equations can be written based on Figure 4(a). The voltage on the primary and secondary sides of the dual coupled inductors are showed as

$$2nV_s^I = V_L - V_p^I + V_{c1} + V_{c2} - V_H \quad (12)$$

$$2nV_p^I = V_L - V_p^I + 4nV_L - V_H \quad (13)$$

$$V_p^I = \frac{(1+4n)V_L - V_H}{1+2n} \quad (14)$$

The voltage on the primary and secondary sides of the dual coupled inductors in mode II can be written based on Figure 4(b):

$$V_p^{II} = V_L \quad (15) \quad V_s^{II} = nV_p^{II} = nV_L \quad (16)$$

Thus, the voltage of capacitors  $C_2$  and  $C_3$  is also derived on Fig. 4(b). The voltage is expressed as

$$V_{c1} = V_{c2} = 2V_s^I = 2nV_L \quad (17)$$

Using the volt-second balance principle on the magnetizing inductor  $L_m$ , the following is given:

$$\int_0^{DT_s} V_p^I dt + \int_{DT_s}^{T_s} V_p^{II} dt = 0 \quad (18)$$

Substituting (12) and (13) into (16), the voltage gain of the buck-mode operation is obtained as

$$M_{\text{buck}} = \frac{V_L}{V_H} = \frac{D}{1+2n+2nD} \quad (19)$$

### 4. Simulation Results

To illustrate the performance and the functions of the proposed converter, this converter is implemented in the MATLAB. The specifications are:

- 1) dc voltage  $V_L$  is 24 V and  $V_H$  is 400 V;
- 2) output power: 200 W;
- 3) switching frequency: 50 kHz;
- 4) Coupled inductor:  $N_p : N_s = 1 : 3$ ,  $L_m = 120 \mu\text{H}$ ;
- 5) Capacitors  $C_1$  and  $C_2$  is 470  $\mu\text{F}$ ;
- 6) MOSFETs  $S_1, S_2, S_3, S_4$ : IRFP4568PBF;  $S_5, S_6$ : IXFK64N50P;  $S_7$ : IXFK64N60P;

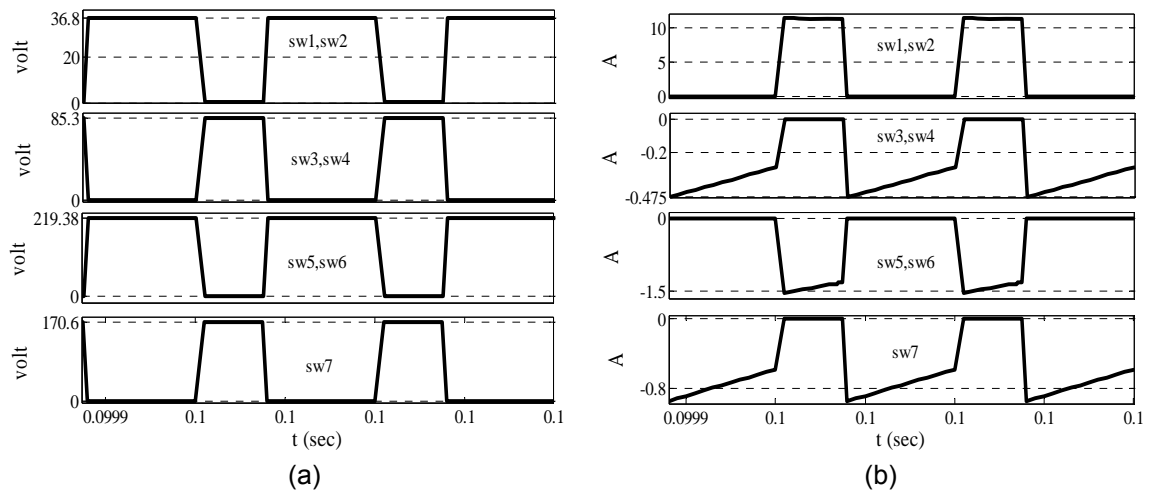


Figure 5. Experiment results in the boost mode under full load  $P_o = 200$  W. (a) voltage stress of switches, (b) current of switches.

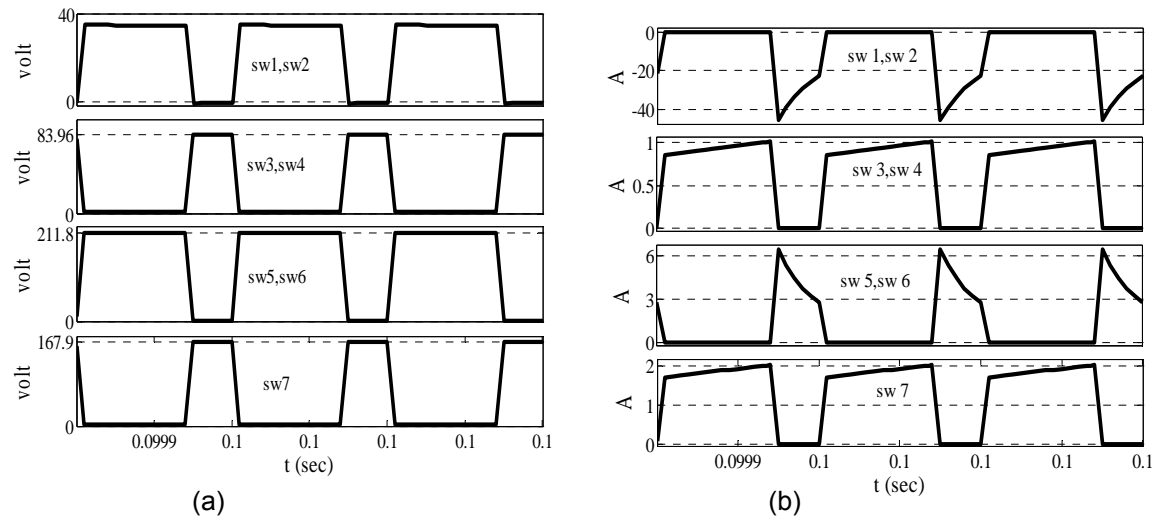


Figure 6. Experiment results in the buck mode under full load  $P_o = 200$  W. (a) voltage stress of switches, (b) current of switches.

In Figure (5), the waveforms are the boost mode operation at full load  $P_o = 200$  W,  $V_{in} = 24$  V, and  $V_{out} = 400$  V. The waveforms illustrate that the steady-state analysis of the boost mode is correct. According to (11) and specifications, the duty cycle is 34.5%. Figure 5(a) illustrates waveform of voltage stress of switches. According to (10) stress voltage of main switches  $S_1, S_2$  equal in 36.65 V. Because the proposed converter works in the boost mode, stress voltage in low side switch  $S_1, S_2$  reduced. Figure 5(b) illustrates waveform of current of switches. Because the proposed converter works in the boost mode, stress voltage in low side switches  $S_1, S_2$  reduced.

In Figure (6), the waveforms are the buck mode operation at full load  $P_o = 200$  W,  $V_{in} = 400$  V, and  $V_{out} = 24$  V. According to (19) and specifications, the duty cycle is 65.5%. Figure 6(a) illustrates waveform of voltage stress of switches. Stress voltage of main switch  $S_7$  is 165 V. Figure 6(b) illustrates waveform of current of switches. Because the proposed converter works in the buck mode, stress voltage in high side switch  $S_7$  reduced.

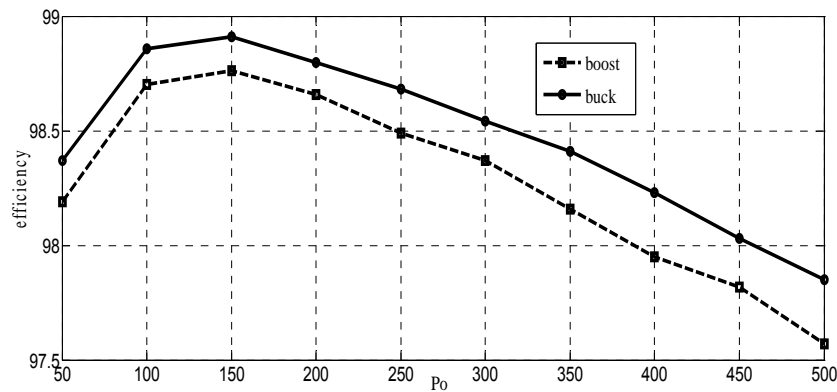


Figure 7. Experimental efficiency in the boost and buck mode

Figure (7) shows the measured efficiency of proposed converter in boost and buck mode at  $V_L = 24\text{ V}$  and  $V_H = 400\text{ V}$ . The maximum efficiency in the boost mode is 98.76% at  $P_o = 150\text{ W}$  and full load efficiency is 98.66% at  $P_o = 200\text{ W}$ . The maximum efficiency in the buck mode is 98.91% at  $P_o = 150\text{ W}$  and full load efficiency is 98.8% at  $P_o = 200\text{ W}$ .

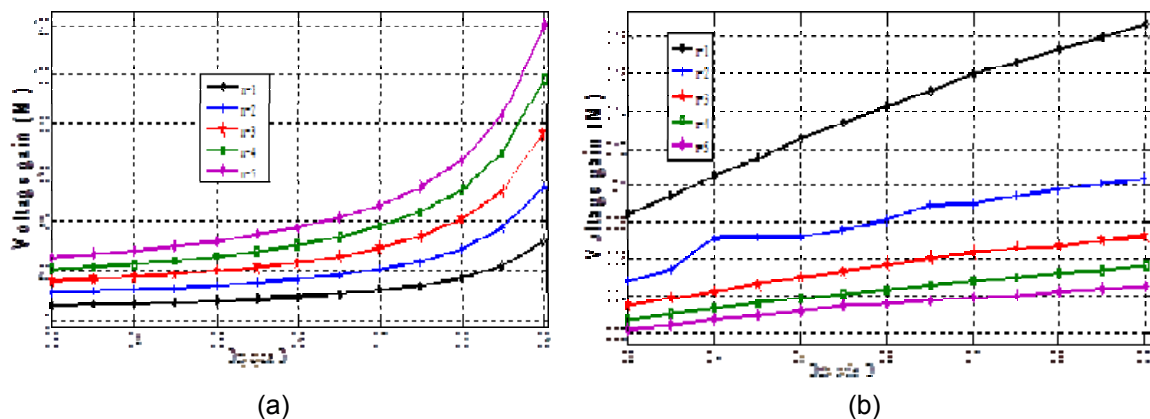


Figure 8. Voltage gain curves under different turn ratio. (a) boost mode, (b) buck mode.

Figure (8) shows the voltage gain versus the duty cycle under various turns ratio of coupled inductors in the boost mode. In the boost mode, if the turn ratio increases, voltage gain will also be increased.

Figure (9) shows the voltage gain versus the duty cycle under various turns ratio of coupled inductors in the buck mode. In the buck mode, if the turn ratio increases, voltage gain will be decreased.

## 5. Conclusion

This paper has proposed a high-efficiency, and high step-up and step-down bidirectional dc-dc converter. This converter successfully developed a high-voltage gain bidirectional dc-dc converter by input-parallel output-series in the boost mode and input-series output-parallel in the buck mode. By using the two capacitors charged in parallel and discharged in series by the dual coupled inductors, high conversion ratio and high efficiency has been achieved. The voltage gain increased by using a dual coupled inductor with a low turn ratio. Simulation results show that the efficiency at full load  $P_o = 200\text{ W}$  is 98.66% in the boost mode and 98.8% in the buck mode.

## References

- [1] C Cecati, F Ciancetta, and P Siano. "A multilevel inverter for photovoltaic systems with fuzzy logic control". *IEEE Trans. Ind. Electron.* 2010; 57(12): 4115–4125.
- [2] Ghadimi, Noradin. "Using HBMO Algorithm to Optimal Sizing & Siting of Distributed Generation in Power System". *Bulletin of Electrical Engineering and Informatics* 3. 2014; 1.
- [3] R Seyezhai, HarineeHarinee, Nagarajan Nagarajan. "Simulation and Implementation of Soft-Switched Interleaved DC-DC Boost Converter for Fuel Cell Systems". *BEEI.* 2012; 1(3).
- [4] JY Lee and SN Hwang. "Non-isolated high-gain boost converter using voltage-stacking cell". *Electron. Lett.* 2008; 44(10): 644–645.
- [5] R Seyezhai, R Anitha, S Mahalakshmi, M Bhavani. "High Gain Interleaved Boost Converter for Fuel Cell Applications". *BEEI.* 2013; 2(4).
- [6] Luiz Henrique SC Barreto, Paulo Peixoto Praca, Demercil S Oliveira Jr, and Ranoyca NAL Silva. "High-voltage gain boost converter based on three-state commutation cell for battery charging using PV panels in a single conversion stage". *IEEE Trans. Power Electron.* 2014; 29(1): 150–158.
- [7] Nagulapati Kiran. "Sliding Mode Control of Buck Converter". *BEEI.* 2014; 3(1).
- [8] R Gules, JDP Pacheco, HL Hey, and J Imhoff. "A maximum power point tracking system with parallel connection for PV stand-alone applications". *IEEE Trans. Ind. Electron.* 2008; 55(7): 2674–2683.
- [9] Ghadimi N. An adaptive neuro-fuzzy inference system for islanding detection in wind turbine as distributed generation. Complexity.doi: 10.1002/cplx.21537. 2014.
- [10] RY Duan and JD Lee. "High-efficiency bidirectional dc–dc converter with coupled inductor". *IET Power Electron.* 2012; 5(1): 115–123.
- [11] H Tao, JL Duarte, and MAM Hendrix. "Line-interactive UPS using a fuel cell as the primary source". *IEEE Trans. Ind. Electron.* 2008; 55(8): 3012–3021.
- [12] YP Hsieh, JF Chen, TJ Liang, LS Yang. "Novel high step-up DC-DC converter for distributed generation system". *IEEE Trans. Ind. Electron.* 2013; 60(4): 1473–1482.
- [13] Venkatesan K. 'Current mode controlled bidirectional flybackconverter'. Proc. IEEE PESC. 1989: 835–842.
- [14] Chen G, Lee YS, Hui SYR, Xu D, Wang Y. 'Actively clamped bidirectional flyback converter'. *IEEE Trans. Ind. Electron.* 2000; 47(4): 770–779.
- [15] Huber L, Jovanovic MM. 'Forward-flyback converter with current-doubler rectifier: analysis, design, and evaluation results'. *IEEE Trans. Power Electron.* 1999; 14(1): 184–192.
- [16] Zhang F, Yan Y. 'Novel forward-flyback hybrid bidirectional DC–DC converter'. *IEEE Trans. Ind. Electron.* 2009; 56(5): 1578–1584.
- [17] Li H, Peng FZ, Lawler JS. 'A natural ZVS medium-power bidirectional DC–DC converter with minimum number of devices'. *IEEE Trans. Ind. Appl.* 2003; 39(2): 525–535.
- [18] Peng FZ, Li H, Su GJ, Lawler JS. 'A new ZVS bidirectional DC–DC converter for fuel cell and battery Application'. *IEEE Trans. Power Electron.* 2004; 19(1): 54–65.
- [19] Lin BR, Huang CL, Lee YE. 'Asymmetrical pulse-width modulation bidirectional DC–DC converter'. *IET Power Electron.* 2008; 1(3): 336–347.
- [20] Mi C, Bai H, Wang C, Gargies S. 'Operation, design and control of dual H-bridge-based isolated bidirectional DC–DC converter'. *IET Power Electron.* 2008; 1(4): 507–517.
- [21] Khan FH, Tolbert LM, Webb WE. 'Hybrid electric vehicle power management solutions based on isolated and nonisolated configurations of multilevel modular capacitor-clamped converter'. *IEEE Trans. Ind. Electron.* 2009; 56(8): 3079–3095.
- [22] Monge SB, Alepuz S, Bordonau J. 'A bidirectional multilevel boost–buck DC–DC converter'. *IEEE Trans. Power Electron.* 2011; 26(8): 2172–2183.
- [23] Peng FZ, Zhang F, Qian Z. 'A magnetic-less DC–DC converter for dual-voltage automotive systems'. *IEEE Trans. Ind. Appl.* 2003; 39(2): 511–518.
- [24] Lee YS, Chiu YY. 'Zero-current-switching switched-capacitor bidirectional DC–DC converter'. *IEE Proc. Inst. Elect. Eng. Electr. Power Appl.*, 2005; 152(6): 1525–1530.
- [25] Ko YP, Lee YS, Chao WH. 'Analysis, design and implementation of fuzzy logic controlled quasi-resonant zero-current switching switched-capacitor bidirectional converter'. *IET Power Electron.* 2011; 4(6): 683–692.
- [26] X Hu, Ch Gong. "A High Gain Input-Parallel Output-Series DC/DC Converter with Dual Coupled-Inductors". *IEEE Trans, Ind, Electron.* 2014; 50(1).